Landscape and Urban Planning 177 (2018) 114–127

Contents lists available at ScienceDirect

Landscape and Urban Planning

journal homepage: www.elsevier.com/locate/landurbplan

Research Paper

Analyzing horizontal and vertical urban expansions in three East Asian megacities with the SS-coMCRF model

Weixing Zhang[a,b,c], Weidong Li[a], Chuanrong Zhang[a,b,*], Dean M. Hanink[a], Yueyan Liu[d], Ruiting Zhai[a,b]

[a] Department of Geography, University of Connecticut, Storrs, CT 06269-4148, USA
[b] Center for Environmental Science and Engineering, University of Connecticut, Storrs, CT 06269-4148, USA
[c] Connecticut State Data Center, University of Connecticut, Storrs, CT 06269-4148, USA
[d] Department of Land Resources Management, China University of Geosciences, Wuhan, Hubei 430074, China

ARTICLE INFO

Keywords:
Spatial pattern
Vertical urban expansion
Horizontal urban expansion
Urbanization footprint

ABSTRACT

A recently proposed method based on the spectral similarity-enhanced Markov chain random field cosimulation (SS-coMCRF) model has provided a practical approach for estimating both horizontal and vertical urban expansion of megacities using Landsat images. Estimating vertical urban growth – the area change of mid-rise or taller buildings (MTBs) – makes it possible to gain some new insights into the urban expansion of megacities. This study makes use of the new approach to examine the horizontal and vertical urban expansion of three capital megacities (Beijing, Seoul, and Tokyo) in East Asia during the late 1980s to the mid-2010s. In contrast to previous studies that only assessed horizontal urban growth, which usually showed almost no increase in urban area in some highly developed cities, this study indicates some different findings: (1) Both horizontal and vertical urban expansion had been happening in the three megacities during the studied period, especially with respect to vertical urban expansion. During the studied period there were 20.7 km^2, 11.3 km^2, and 6.8 km^2 MTB area increases in Beijing, Seoul, and Tokyo, respectively. (2) Different cities showed some differences in growth patterns, mainly because they were at different urban development stages and impacted by different local situations in terms of geography, population, and development policies. (3) A similarity is that the three megacities all tended to horizontally expand initially and then grow vertically in the already developed areas. This study may provide a useful new perspective on the urban expansion of megacities.

1. Introduction

The number of megacities across the world increased 10–36 between 1990 and 2016 (United Nations, 2015). One third of these megacities are located in East Asia, with 248 million dwellers. East Asia (including the countries and regions of China, Hong Kong, Japan, Macau, Mongolia, North Korea, South Korea, and Taiwan) is one of the world's rapidly urbanizing regions, with almost 20 million people moving into urban areas every year during the time period between 2000 and 2010 (Frolking, Milliman, Seto, & Friedl, 2013; World Bank Group, 2015). Because of the constant flow of people into urban areas in this region every year, continuing rapid urbanization is expected (Angel, Parent, Civco, Blei, & Potere, 2011). Urbanization has resulted in many socio-economic and environmental problems (Chung, Choi, & Yun, 2004; Civerolo et al., 2007; Kim, 2010; Kim & Kim, 2011; Lee & Choe, 2011). Therefore, governments across the world have been taking strict measures to regulate urban expansion. However, restraining urban growth may not always yield positive results because the real problem is the pattern of growth rather than growth itself (Cho, 2002). Urban forms and spatial patterns significantly impact socio-economic, political, and urban environmental conditions (Alberti, 2005; Kontgis et al., 2014; Luck & Wu, 2002; Schneider, Chang, & Paulsen, 2015; Schneider et al., 2015; Stone, 2008; Sung & Oh, 2011). It is the socio-economic system and the stage of urban development that make urban areas and their spatial patterns clearly different amongst different regions and countries (Bagan & Yamagata, 2014; Murakami, Zain, Takeuchi, Tsunekawa, & Yokota, 2005; Schneider & Mertes, 2014). For example, urban residents in East Asia are more likely to live in mid-rise or taller buildings (MTBs) that are as close to urban centers as possible, while urban dwellers in North America generally tend to live in single family houses in suburban areas (Bagan & Yamagata, 2014). Therefore, it is important to understand the particular spatial patterns of urban growth in the megacities of East Asia for better city planning and urban sustainability research (Han, Hayashi, Cao, & Imura, 2009).

* Corresponding author at: Department of Geography, University of Connecticut, Storrs, CT 06269-4148, USA.
E-mail address: chuanrong.zhang@uconn.edu (C. Zhang).

https://doi.org/10.1016/j.landurbplan.2018.04.010
Received 15 November 2017; Received in revised form 15 March 2018; Accepted 28 April 2018

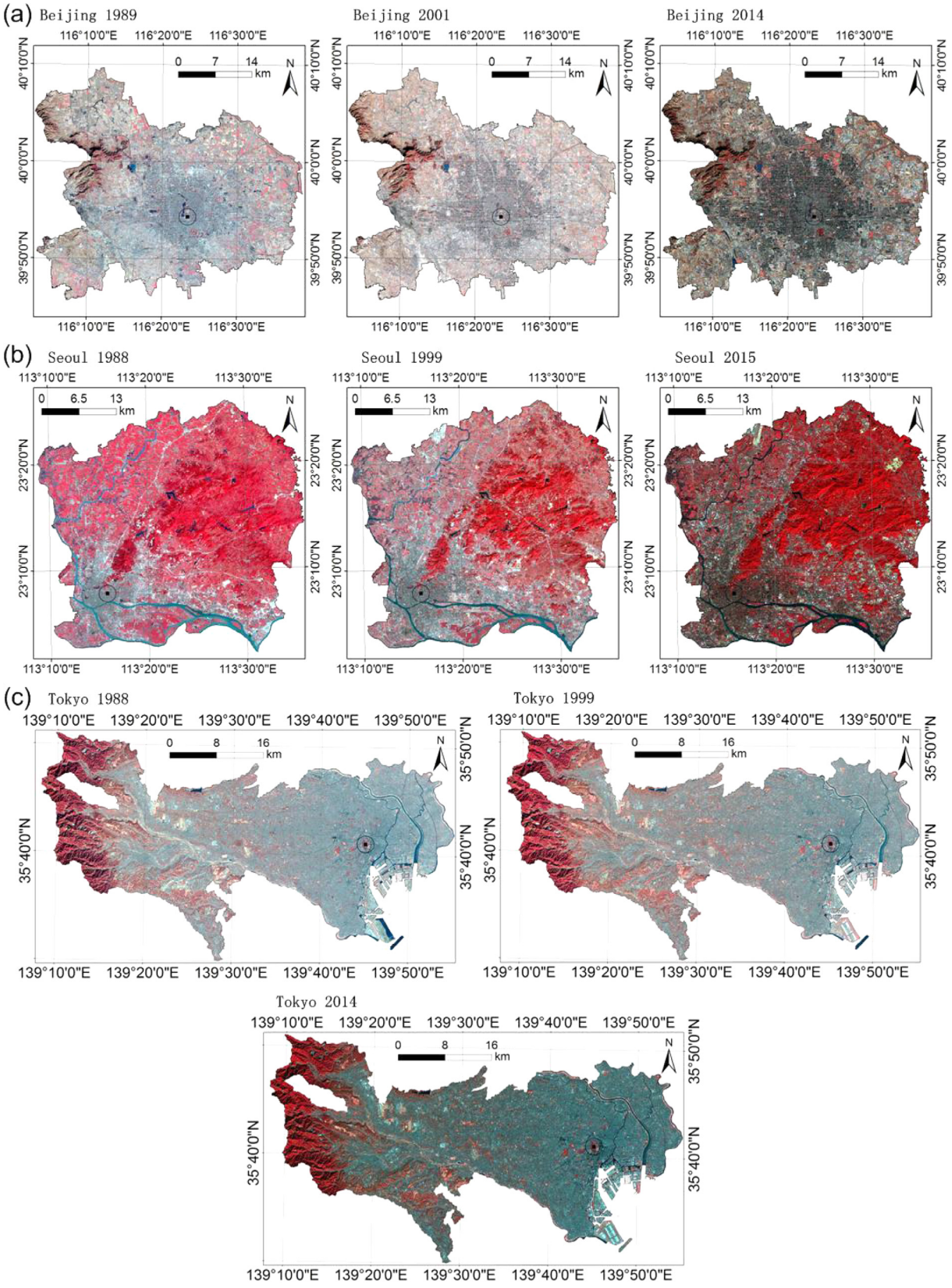

Fig. 1. The Landsat false color images for (a) Beijing, (b) Seoul, and (c) Tokyo at three time points during the studied period from the late 1980s to the mid-2010s.

Remote sensing (RS) technology has been a powerful tool to study urbanization (Montgomery, 2008; Schneider, 2012). Many analyses on urban growth, particularly horizontal urban growth, have been conducted using a variety of spatial analysis methods, RS techniques, and data at various scales. At the global scale, Huang, Lu, and Sellers (2007) compared the urban forms of 77 metropolitan areas all over the world. Angel et al. (2011) mapped all cities with a population of more than 100,000 in 2000 and then projected the urban areas from 2000 to 2050.

Table 1
Description of selected megacities.

City name	Study area (km^2)	Population (10^6 persons by year)			Names of selected districts for each megacity
		Around 1988	Around 2000	Around 2014	
Beijing	1364.28	6.45	8.69	12.76	Dongcheng, Xicheng, Haidian, Chaoyang, Fengtai, and Shijingshan
Seoul	606.97	10.90	10.28	10.30	Gangdong, Songpa, Gangnam, Seocho, Gwanak, Dongjak, Yeongdeungpo, Geumcheon, Guro, Gangseo, Yangcheon, Mapo, Seodaemun, Eunpyeong, Nowon, Dobong, Gangbuk, Seongbuk, Jungnang, Dongdaemun, Gwangjin, Seongdong, Yongsan, Jung, and Jongno
Tokyo	1402.32	11.75	11.98	13.29	Chiyoda, Chuo, Minato, Shinjuku, Bunkyo, Taito, Sumida, Koto, Shinagawa, Meguro, Ota, Setagaya, Shibuya, Nakano, Suginami, Toshima, Kita, Arakawa, Itabashi, Nerima, Adachi, Katsushika, Edogawa, Hachioji, Tachikawa, Musashino, Mitaka, Ome, Fuchu, Akishima, Chofu, Machida, Koganei, Kodaira, Hino, Higashimurayama, Kokubunji, Kunitachi, Fussa, Komae, Higashiyamato, Kiyose, Higashikurume, Musashimurayama, Tama, Inagi, Hamura, Akiruno, and Nishitokyo

In Taubenböck et al. (2012), the urbanization of 27 megacities across the world was mapped and analyzed across a time period of about 40 years. At the regional scale, Taubenböck, Wegmann, Roth, Mehl, and Dech (2009) measured and analyzed the urban footprints of the 12 largest urban agglomerations in India using absolute indices and landscape metrics. By comparing the area changes of impervious surfaces in megacities in China and the U.S.A., Kuang, Chi, Lu, and Dou (2014) found that infilling mainly occurred in megacities in the U.S.A., while edge-expansion is the dominant form of urban expansion in Chinese cities. At the local scale, Hara, Takeuchi, and Okubo (2005) investigated the micro-scale transformation from agricultural landscape to urban landscape in Bangkok using aerial photographs. Yu and Ng (2007) applied an integrated method of landscape metrics and gradient analysis to assess the spatiotemporal changes of urban expansion with a case study of Guangzhou. Hung, Chen, and Cheng (2010) quantitatively compared the urban land cover patterns of Tokyo, Kyoto, and Taipei with ALOS RS data. Taubenböck et al. (2014) tracked the urbanization process of the Hong Kong-Shenzhen-Guangzhou mega-region with the use of spatial metrics.

Some studies have been conducted to detect vertical urban expansion using high resolution RS images. For example, multi-temporal very-high resolution (VHR) RS images were used to identify changes of individual buildings (Doxani, Karantzalos, & Tsakiri-Strati, 2012; Leichtle, Geiß, Wurm, Lakes, & Taubenböck, 2017; Pan, Zhao, Chen, Liang, & Sun, 2008). Yu, Liu, Wu, Hu, and Zhang (2010) developed an automatic object-based method to identify building objects and extract various building information based on high-resolution airborne LiDAR data. Zhang (2015) extracted three-dimensional (3-D) building information from Quickbird images to investigate the change of urban 3-D morphology. However, previous studies of urban change analysis the highest resolution images of individual buildings remain limited for previous studies of urban change analysis due to only recent data availability, and at the same time they remain at the level of small-area case studies. In addition, only a few studies of spatial pattern analysis of urbanization considered both horizontal and vertical urban expansion. For example, Wurm, Taubenböck, Esch, Fina, and Siedentop (2013) combined historical two-dimensional (2-D) urban change and a current 3-D city model derived from LiDAR to analyze the relationship between horizontal urban growth and vertical urban growth, but with a limitation that vertical urban expansion can only be measured in areas that have been part of horizontal urban expansion. Salvati, Zitti, and Sateriano (2013) identified the spatial pattern of urban growth in the Athens metropolitan area, which has been shifting from vertical growth to horizontal growth since the 1990s, using building height survey records. Frolking et al. (2013) used DMSP/OLS nighttime light data for measuring horizontal urban growth and used SeaWinds microwave backscatter power return data for detecting vertical urban growth in 100 cities worldwide.

Recently, based on the spectral similarity-enhanced Markov chain random field cosimulation (SS-coMCRF) model for land cover post-classification (Li et al., 2015; Zhang, Li, Zhang, & Li, 2017), Zhang, Li, Zhang, and Ouimet (2017) further proposed an integrated framework for detecting both horizontal and vertical urban expansion using medium resolution Landsat images, with an overall identification accuracy of 78% in a case study of Guangzhou. The vertical urban expansion was represented by the detected area of MTBs based on their shadows in Landsat images. By utilizing the integrated framework, this study aims to explore and analyze the spatial patterns of horizontal and vertical urban expansion of three megacities in East Asia: Beijing, Seoul, and Tokyo, from the late 1980s to the mid-2010s. The intention of this study is to provide some answers to the following questions: (1) Has the urban growth of megacities in East Asian developed countries stagnated? (2) What are the similarities and differences in spatial patterns of horizontal and vertical urban growth between the studied megacities? The main novelties of this study are that (1) it provides some new historical information and insight about the urban expansion of three megacities in East Asia (i.e., Beijing, Tokyo, and Seoul) from the perspective of vertical urban expansion, and (2) it also provides a practical experiment of conducting horizontal and vertical urban change analysis at the scale level of a megacity over a long time period (approximately 30 years).

2. Study areas and data

2.1. Study areas

Three megacities were chosen for this study from East Asian countries: Beijing, Seoul, and Tokyo (Fig. 1). These megacities, as defined by administrative boundaries, were investigated in order to match corresponding demographic and geographical data (Table 1). Beijing is the capital of China, located in the North China Plain. It includes six main urban districts and ten suburban and rural districts. The main urban area of Beijing (i.e., the six main urban districts) was selected for our analysis. It had a population of 12.76 million over a land area of 1364.28 km^2 in 2014 (Beijing Statistical Bureau, 2015). Seoul is the capital and the most populous city of South Korea. It includes twenty-five districts. It has a population of 10.30 million, accounting for around 20% of the total population of South Korea, with a land area of 606.97 km^2 (Seoul Statistics, 2016). The entire area was selected for our analysis. As the capital and the most populous city of Japan, Tokyo consists of the city of Tokyo, Tama Area, Nishi-Tama District, and Islands. Twenty-three special wards of the city of Tokyo and twenty-six cities of the Tama Area were selected as our study area, with the total population exceeding 13.29 million and a land area of 1402.32 km^2 (Statistics of Tokyo, 2016). These three study areas were selected because they are among the largest megacities in East Asia and also represent megacities at different urbanization stages (i.e., Beijing is in the stage of fast urbanization; Seoul is in the stage of reurbanization; Tokyo is in the stage of suburbanization). Analyzing the spatial patterns of horizontal and vertical urban expansion can provide valuable insights for urban planning and urban sustainability of current and potential megacities in East Asia.

Table 2
Description of used Landsat images and corresponding expert-interpreted land cover sample data.

City name	Landsat sensor type	Image acquisition date	Path	Row	Sun elevation angle (°)	Sun azimuth angle (°)	Sample data (pixel labels)
Beijing	Landsat 5 TM	11/18/1989	123	32	26.0	153.4	4787
	Landsat 7 ETM +	12/29/2001	123	32	22.9	156.8	4039
	Landsat 8 OLI	12/25/2014	123	32	23.8	160.1	6094
Seoul	Landsat 5 TM	11/14/1988	116	34	29.8	153.4	3517
	Landsat 7 ETM +	01/29/2002	116	34	29.1	150.7	3743
	Landsat 8 OLI	12/27/2015	116	34	26.1	158.8	3528
Tokyo	Landsat 5 TM	12/01/1988	107	35	27.3	153.2	3717
	Landsat 7 ETM +	12/08/1999	107	35	28.1	158.4	4177
	Landsat 8 OLI	12/09/2014	107	35	28.7	160.1	4377

2.2. Data

Spatial data used in this study include geographic information system (GIS) data, RS data, and expert-interpreted data. GIS data are administrative boundary shapefiles for study areas. We obtained the administrative boundary shapefiles of Beijing and Seoul from ArcGIS (https://www.arcgis.com/home/item.html), and the shapefile of Tokyo from National Land Numerical Information Download Service of Japan (http://nlftp.mlit.go.jp/ksj-e/gml/gml_datalist.html). All of these GIS data were checked and corrected if there were mistakes or some information was missing. Finally, only selected districts of each megacity were merged as the corresponding study area.

In this study, three sets of Landsat series images were acquired via the EarthExplorer from U.S. Geological Survey (http://earthexplorer.usgs.gov/), among which each set has three scenes selected for around 1988, around 2000, and around 2014, acquired by Landsat 5 TM sensor, Landsat 7 Enhanced Thematic Mapper Plus (ETM +) sensor, and Landsat 8 Operational Land Imager (OLI) sensor, respectively (Fig. 1, Table 2). For each scene, six commonly used channels, blue, green, red, near infrared (NIR), short-wave infrared 1 (SWIR 1), and short-wave infrared 2 (SWIR 2), were composited and used for pre-classification (note that pre-classification is one of the required steps for using the SS-coMCRF-based integrated framework for detecting both horizontal and vertical urban expansion, as explained in the Section 3). Four land cover classes (built-up area, vegetation, bare land, and waterbody) were considered, besides the shadow class in pre-classification stage, along the lines of Zhang, Li, Zhang, and Ouimet (2017).

As a MCRF-based model, the use of SS-coMCRF for performing post-classification requires expert-interpreted data. Therefore, an expert-interpreted sample dataset of pixel labels for the four land cover classes (i.e., built-up area, vegetation area, waterbody, and bare land) was discerned for each study area at each time point (Li et al., 2015; Zhang, Li, & Zhang, 2016; Zhang, Li, Zhang, & Li, 2017). Correspondingly, nine expert-interpreted sample datasets were obtained from the selected Landsat images and other data sources (e.g., Google Earth history imagery), as given in Table 2. Please note that expert-interpreted sample data are different from training data for pre-classification because they were interpreted from multiple sources instead of only the corresponding optical RS images used for pre-classification. Correctness is the major concern for expert-interpreted sample data for post-classification. However, reflecting the spectral situations of land cover classes in the RS images for pre-classification is the major concern for training data. Additional details concerning expert-interpreted sample data can be found in Li et al. (2015), Zhang et al. (2016), and Zhang, Li, Zhang, and Li (2017). The validation data are also expert-interpreted sample data, and they are used for overall accuracy assessment of all land cover classes.

3. Methods

3.1. The SS-coMCRF-based integrated framework

The SS-coMCRF-based integrated framework (Zhang, Li, Zhang, & Ouimet, 2017) has shown to be one (and possibly the only) effective method for detecting both horizontal and vertical urban growth from medium resolution imagery, with valuable detection results at the megacity scale. The SS-coMCRF model (Zhang, Li, Zhang, & Li, 2017) is an extension of the Markov chain random field cosimulation (coMCRF) model (Li et al., 2015) based on the Markov chain random field (MCRF) theory (Li, 2007; Li & Zhang, 2008). It was developed for reducing the smoothing effect of the coMCRF model for improving land cover classification as a land cover post-classification method (Zhang et al., 2016). As detailed in the flowchart of Fig. 2, the integrated framework comprises the following major steps (Zhang, Li, Zhang, & Ouimet, 2017): pre-classification, post-processing, shadow detection, MTB estimation, accuracy assessment, and change analysis:

(1) Pre-classification. The widely-used support vector machine (SVM) classifier was used in this study to produce pre-classified images from the Landsat images. The shadow class and the waterbody class were then merged as one waterbody class in the pre-classified images for further post-classification operations using the SS-coMCRF model.
(2) Post-processing. The SS-coMCRF model was used to perform post-classifications to improve the pre-classified land cover data by integrating expert-interpreted data, spatial correlation information, and pre-classified land cover data together through MCRF cosimulation. In this study, 100 simulated realizations were produced in each post-classification operation, and then an optimal classification map was further obtained based on the maximum probabilities estimated from the 100 simulated realizations. The expert-interpreted validation data was used to estimate the accuracy of the optimal classification map in order to make sure it was accurate enough for shadow detection in the next step.
(3) Shadow detection. Shadow detection is based on an assumption that waterbodies from pre-classification which are present in built-up areas from post-classification are supposed to be shadows. During pre-classification, most shadows are usually misclassified as waterbodies because of spectral confusion between what constitutes a shadow versus a waterbody, particularly in the central area of a large city where more MTBs exist. A majority of those misclassifications are corrected after post-processing with SS-coMCRF. By overlap analysis, shadows misclassified in the pre-classification step are distinguished from waterbodies: First, all waterbodies in a pre-classified image are extracted as the waterbody class. Second, each waterbody object is then reclassified as a shadow object if it is located in the built-up areas of the corresponding post-classification map.
(4) MTB estimation. A morphological operator based on spatial logic

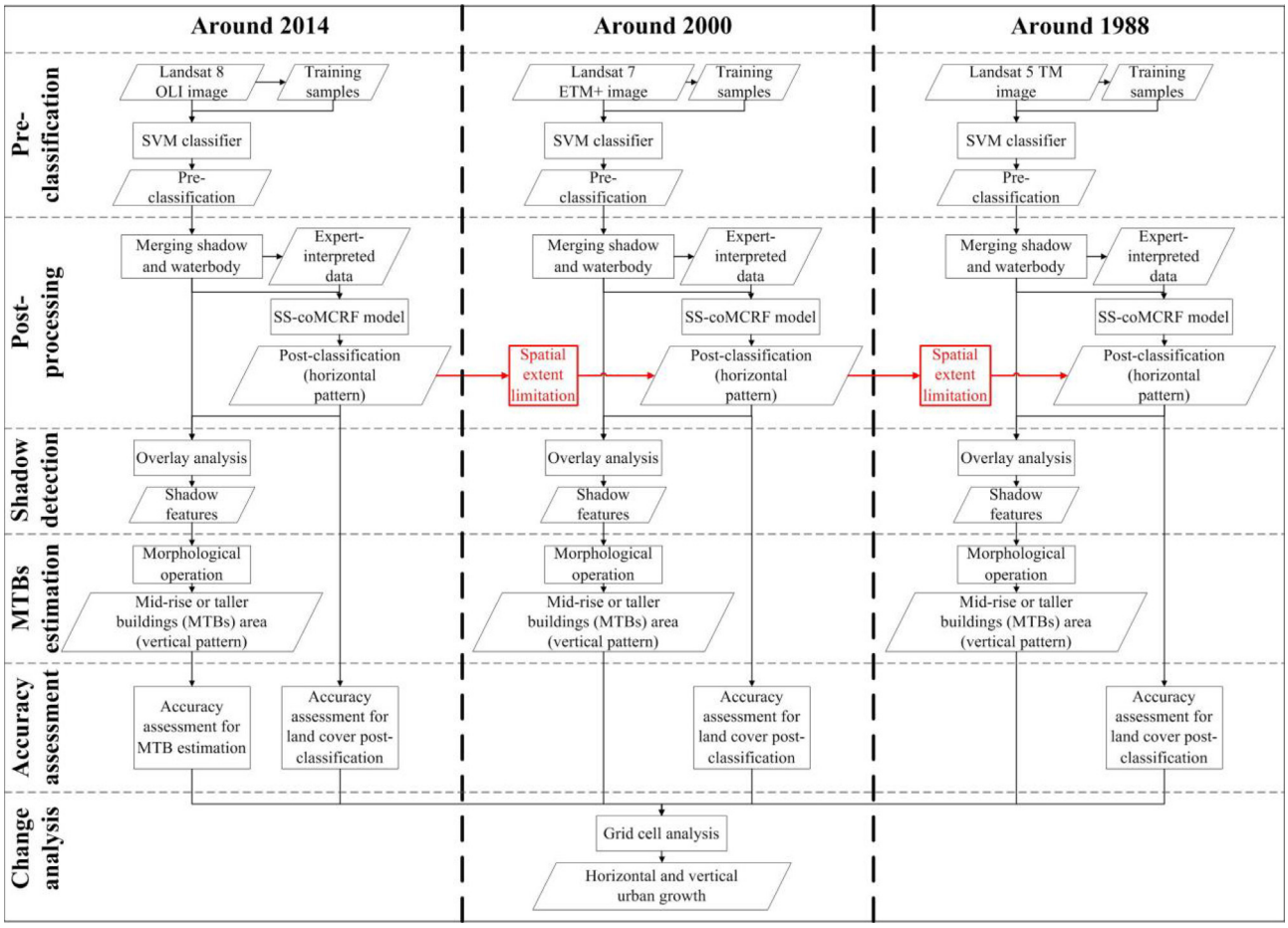

Fig. 2. A flowchart for illustrating the whole process of detecting and analyzing horizontal and vertical urban growth performed in this study.

reasoning was used to estimate high-rise building areas from detected shadows from the last step according to the spatial relationships among the sun, the satellites, and the buildings. The idea of this morphological operator is to construct the spatial logic relationship between a shadow and its corresponding MTB; that is, a pixel (or a group of pixels as an object) is considered an MTB if a shadow occurs as its neighbor in the dark side of the building.

(5) Accuracy assessment. A confusion matrix was used to assess the accuracy of each post-classification map with the validation data (also expert-interpreted sample data). Accuracy assessment was only conducted for the 2014 MTB estimation because of the lack of available high resolution imagery. Around 6% of the total estimated MTB areas were selected and manually compared to reference high resolution imagery from multiple sources (including Google Maps, Bing Maps, Baidu Maps, etc.).

(6) Change analysis. Grid cell analysis, a promising method for visualizing urban growth patterns (Bagan & Yamagata, 2012, 2014), was used in this study for analyzing built-up areas, MTBs, urban horizontal growth, urban vertical growth, and their spatial patterns. In order to match the spatial resolution of used channels of Landsat images (i.e., 30 m × 30 m), grid cell analysis was conducted at the resolution of 990 m × 990 m (i.e., 33 × 33 = 1089 Landsat image pixels). By overlaying analysis, the numbers of 30 m × 30 m built-up areas and MTB pixels in each grid cell are counted and the proportion of built-up areas and MTBs are calculated and assigned to the grid cell of the corresponding empty raster data layer. By conducting overlap subtraction between results for different years, horizontal spatial-temporal changes in built-up areas, vertical changes in MTB areas, and the transition from non-MTB areas to MTB areas can be calculated and visualized.

With the use of the integrated framework on the cropped Landsat images, high-quality land cover maps and MTB maps of each study area at three points in time were generated.

In order to minimize the overestimation of urban areas due to mixed pixels and poor image quality, we assumed that built-up areas are always spatially expanding rather than sometimes shrinking (Taubenböck et al., 2012, 2014). Therefore, we modified a post-classification map for an earlier time by judging a built-up area pixel to be true only if the pixel at the same location is in a built-up area in a post-classification map for a later time (Fig. 2: Post-processing). Similarly, vertical urban expansion was assumed to be unidirectional, which means the total number of MTB pixels within a grid cell in an earlier year is always smaller than the total number of MTB pixels within the same cell in a later year. Such treatments eliminated the possible existence of large-scale demolishment of built-up areas and high buildings.

3.2. Gaussian kernel density

In this study, a kernel-density estimation with Gaussian kernels from the Statistical functions in the SciPy module (a Python-based open-source software, see Jones, Oliphant, & Peterson, 2016) was used to visualize and analyze the distributional distance of horizontal and vertical urban growth to a city center, with an automatic bandwidth determination based on Scott's Rule. High Gaussian kernel density indicates a high level of likelihood of a certain amount of urban expansion occurring in a certain distance from a city center, and vice versa.

Kernel density estimation is a well-known way to estimate the probability density function of a random variable in a non-parametric way (Jones et al., 2016; Lampe & Hauser, 2011; Scott, 2015). Given that (x_1, x_2, …, x_n) (x can be a 1-D array or a 2-D array) is a univariate

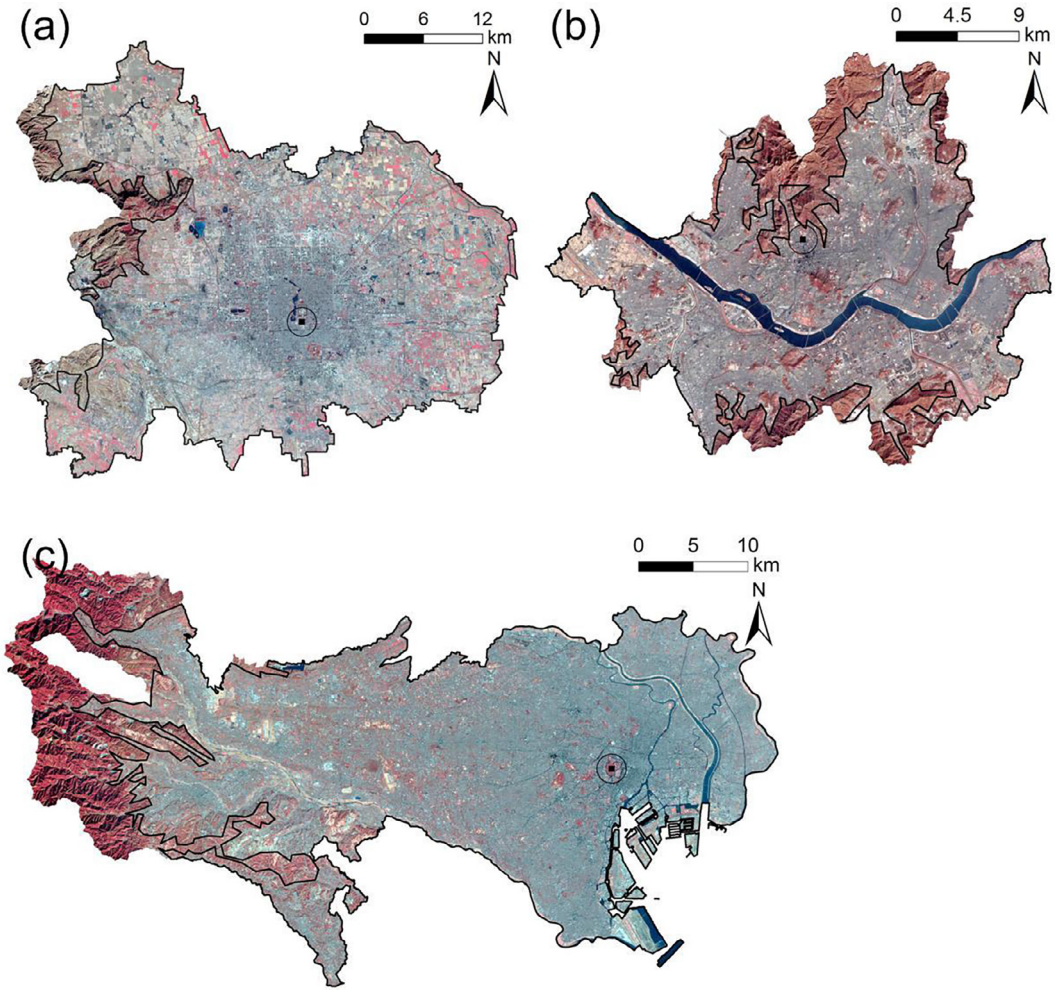

Fig. 3. Boundaries of developable spaces for horizontal and vertical urban expansion in Beijing, Seoul, and Tokyo in the late 1980s. (a), (b), and (c): Landsat false color images with manually-drawn boundaries of developable areas by excluding mountains and waterbodies for Beijing in 1989, Seoul in 1988, and Tokyo in 1988, respectively. (For interpretation of the references to colour in this figure legend, the reader is referred to the web version of this article.)

Table 3
Accuracy assessment for land cover post-classification and MTB estimation.

City name	Year	Number of validation data	Overall accuracy (%)	Kappa coefficient	Correctly classified samples/Total validation samples	Number of estimated MTB patches	MTB accuracy (%)
Beijing	1989	798	74.8	0.632	–	–	–
	2001	674	78.6	0.655	–	–	–
	2014	1015	81.1	0.654	630/676	11,766	93.2
Seoul	1988	502	93.4	0.854	–	–	–
	2002	535	94.6	0.886	–	–	–
	2015	505	94.5	0.873	433/475	7731	91.2
Tokyo	1988	620	93.4	0.876	–	–	–
	1999	697	94.5	0.896	–	–	–
	2014	876	94.4	0.889	271/331	6613	81.9

"–" indicates no available data.

independent and identically distributed sample from a distribution with a density f, the kernel density estimator $\hat{f}_h(x)$ is:

$$\hat{f}_h(x) = \frac{1}{n}\sum_{i=1}^{n} K_h(x-x_i) = \frac{1}{nh}\sum_{i=1}^{n} K\left(\frac{x-x_i}{h}\right) \quad (1)$$

where K is the kernel, a non-negative function that integrates to one; n is the sample size; h is the bandwidth; x is a 2-D array (urban growth, distance to city center).

3.3. Relative frequency distribution

In this study, relative frequency distribution was used to analyze the transition from non-MTB areas to MTB areas, where data variable (m) represents MTB increase in a time period and event (i) represents the percentage range of built-up areas in grid cells at the beginning of the time period (i.e., 0–10%, 10–20%, etc.).

The relative frequency distribution (r) of a data variable (m) is a summary of the frequency proportion in a collection of non-overlapping categories (Yau, 2012):

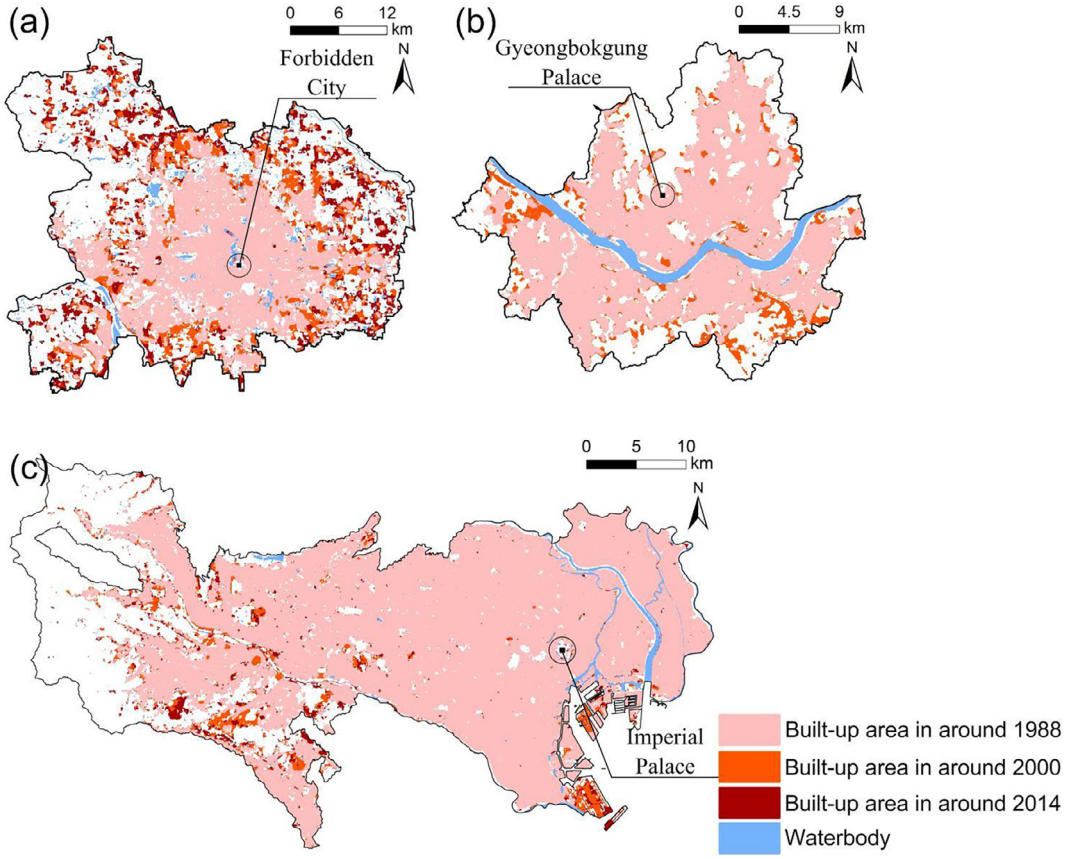

Fig. 4. Horizontal expansion of built-up areas. (a): Beijing from 1989 to 2014; (b): Seoul from 1988 to 2015; (c): Tokyo from 1988 to 2014.

$$r_i = \frac{m_i}{\sum_{i=1}^{n} m_i} \quad (2)$$

where m_i is the value of m for event i; $\sum_{i=1}^{n} m_i$ is the cumulative value of m for all events; n is the total number of events (i.e., 10 in this study, see Fig. 7).

3.4. Developable spaces analysis

To investigate the impact of developable spaces on horizontal and vertical urban growth in each megacity, we manually drew the boundaries of developable areas based on the boundaries of the study areas by excluding mountains and waterbodies (Fig. 3). Developable spaces are usually defined as areas that can be developed into residential, commercial, or other developments under regulations, including open spaces, residential areas, etc. In this analysis, developable spaces for horizontal urban growth include areas of bare land and vegetation; developable spaces for vertical urban growth include built-up areas, bare land, and vegetation, but exclude buffered MTBs (i.e., each MTB and its surrounding one pixel-length buffer area) in built-up areas. A length of one pixel was chosen for the buffer based upon two simplifying assumptions: (1) floor area ratio (FAR) is 100%; (2) all estimated MTB pixels are 10-story buildings, which means each pixel occupies 9 surrounding pixels as the site area for the building. In fact, the heights of buildings vary, which can be 5-stories tall or up to 100-stories tall in estimated MTBs from Landsat images in this study. According to the Japanese Building Standard Law and related regulations, FAR for medium-high residential zones ranges from 100 to 500% and for commercial zones ranges from 200 to 1300%, respectively (Hasegawa, 2013).

4. Results

4.1. Validation

For Seoul and Tokyo, the land cover classification overall accuracies and Kappa coefficients after post-classification are all above 93% and 0.85, respectively (Table 3). Beijing has relatively low land cover classification overall accuracies, ranging from 74.8% to 81.1%, with the corresponding Kappa coefficient ranging from 0.632 to 0.655 (Table 3). This can be explained by the complexity of Beijing's suburban landscapes. For example, in the suburban area of Beijing, urban growth is not always unidirectional as assumed. A large amount of land cover misclassifications in Beijing, caused by the bi-directional conversion between bare land and built-up areas, was observed. Additionally, due to the preparation for the 2008 Beijing Summer Olympics, Beijing transformed a large area of built-up land into green spaces and city parks. Despite this, urban horizontal growth patterns of Beijing are useful, because most of the misclassified shadows (misclassified into waterbodies) in its urban areas were corrected by post-classification for MTB estimation (Zhang, Li, Zhang, & Ouimet, 2017).

About 5–6% of estimated MTB patches were randomly selected for validation. For example, in Beijing, 676 out of the 11,766 estimated MTB patches were chosen and visually validated with reference to high-quality RS images (e.g., ESRI world imagery) (Table 3). The accuracies of detected MTBs around 2014 for the three megacities range from 81.9% to 93.2% (Table 3). The accuracy assessment for MTBs around 1988 and around 2000 was not conducted due to the lack of reference high resolution images. However, their accuracies should be close to the results of around 2014 because of the approximately similar sun elevation angles used for image selection (Zhang, Li, Zhang, & Ouimet, 2017).

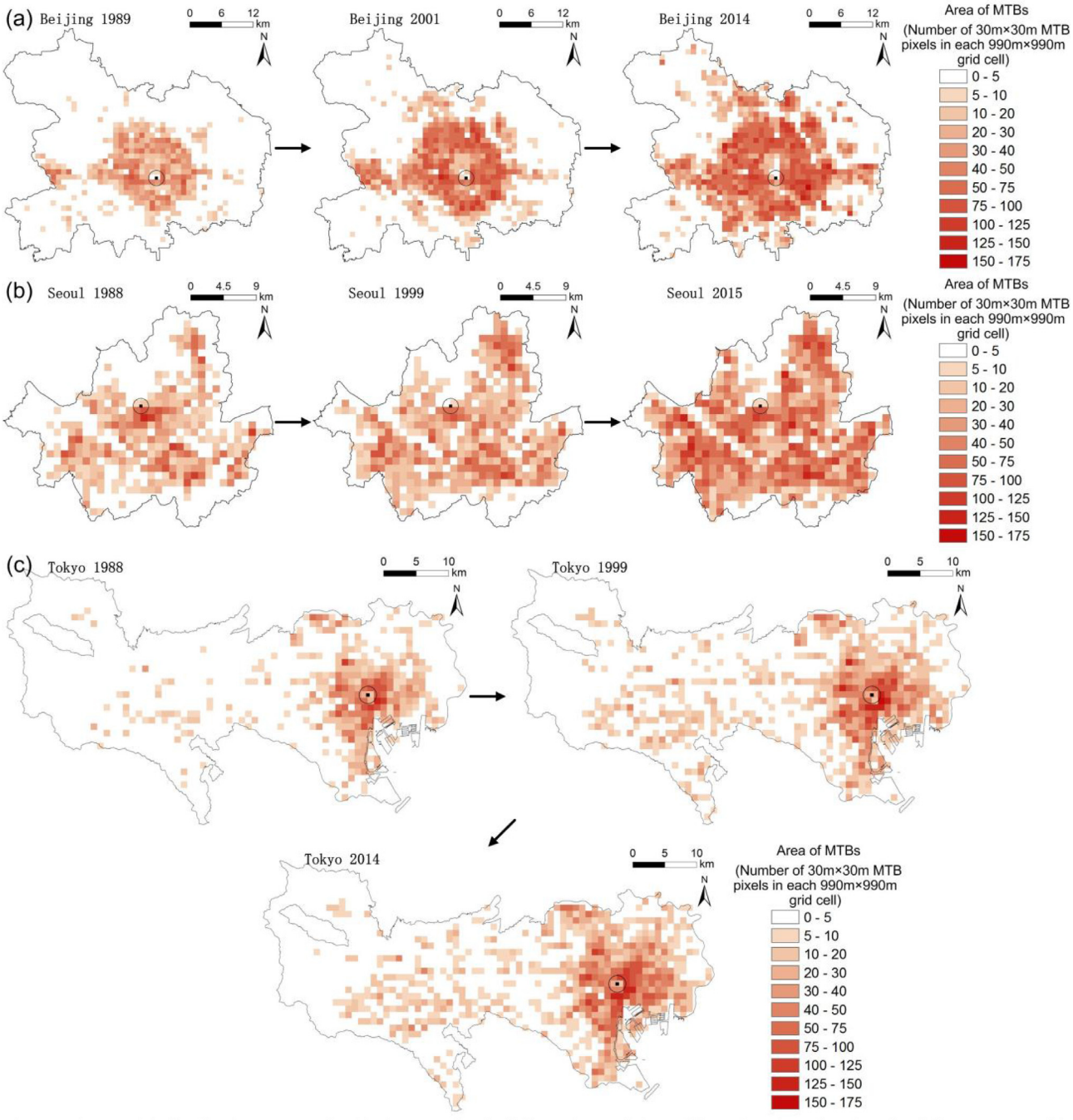

Fig. 5. The spatial distribution maps of mid-rise or taller buildings (MTBs) in Beijing, Seoul, and Tokyo in different years. (a): MTBs in Beijing in 1989, 2001, and 2014; (b): MTBs in Seoul in 1988, 1999, and 2015; (c): MTBs in Tokyo in 1988, 1999, and 2014.

4.2. Horizontal and vertical urban expansion

Fig. 4 shows the horizontal urban growth patterns and urban growth of the three study areas during the late 1980s to the mid-2010s, and Fig. 5 shows the spatial patterns of MTBs in the three study areas on three selected dates during the studied period. For the period from 1989 to 2014, the total estimated built-up area in Beijing increased from 535.36 km^2 to 707.79 km^2, the greatest increment among the studied cities (Table 4). The increase mainly occurred during 2001–2014 in the rural-urban fringes (Fig. 4(a)). With respect to vertical urban growth, 9.77 km^2 and 10.93 km^2 of MTB increases happened in Beijing during 1989–2001 and 2001–2014, respectively, at an average annual change rate of 0.82 km^2/year (Table 4), along with outward horizontal urban sprawl (Fig. 5(a)). Compared to Beijing, Seoul experienced slower horizontal urbanization progress during a similar period, especially in the period from 2002 to 2015 (Table 4), with most of its increase occurring in the western and southeastern outskirts of the city and less of the increase occurring inside the city (Fig. 4(b)). During the studied period of 1988–2015, vertical urban growth in Seoul took place across the whole city from its center to its periphery (Fig. 5(b)), and the vertical growth was particularly fast between 2002 and 2015 (Table 4). In contrast to Beijing and Seoul, Tokyo had relatively stable and small horizontal urban expansion during the studied period (Table 4), which mainly occurred in its western region and southeastern corner (Fig. 4(c)). Most MTB increase in Tokyo took place in its western region and the surrounding areas of the Imperial Palace between 1988 and 1999 (Fig. 5(c) and Table 4).

Table 4
Total areas and area changes of estimated built-up areas and estimated MTBs for Beijing, Seoul, and Tokyo for three selected years.

City name	Year	Built-up areas (km^2)	Area change from previous time (km^2)	Annual change rate (km^2/year)	MTBs (km^2)	Area change from previous time (km^2)	Annual change rate (km^2/year)
Beijing	1989	535.36	–	–	8.22	–	–
	2001	574.73	39.38	3.28	17.99	9.77	0.81
	2014	707.79	133.06	10.24	28.92	10.93	0.84
Seoul	1988	334.23	–	–	7.52	–	–
	2002	363.43	29.20	2.09	10.20	2.68	0.19
	2015	377.60	14.17	1.09	18.82	8.62	0.66
Tokyo	1988	936.47	–	–	7.88	–	–
	1999	977.20	40.73	3.70	12.85	4.97	0.45
	2014	1011.92	34.72	2.31	14.68	1.82	0.12

"–" indicates no available data.

4.3. Spatial analysis

4.3.1. Distributional distance of horizontal and vertical urban growth to city center

In Fig. 6, the intensity diagrams of horizontal and vertical urban growth versus the distance from the corresponding city center (i.e., the Forbidden City in Beijing, Gyeongbokgung Palace in Seoul, and the Imperial Palace in Tokyo) indicate that both built-up areas and MTB areas in the studied megacities increased during the entire study period at different speeds. Overall, Beijing experienced the most intense horizontal and vertical urban growth, with an outward expanding trend which mainly occurred in intermediate areas of the city compared to the other two cities (Fig. 6(a), (d), (g), and (j)). Seoul had a similar pattern as Beijing had, but with less growth and without an obvious outward trend (Fig. 6(b), (e), (h), and (k)). Tokyo experienced the least urban growth but its growth tended to be evenly distributed (Fig. 6(c), (f), (i), and (l)).

To be more specific, in Beijing, built-up areas increased quickly from 5 km distance outward till the peak at around 15 km distance for the period from 1989 to 2001 (Fig. 6(a)), with a large amount of the increase occurring between 10 km and 25 km. In the following years (from 2001 to 2014), a large number of grid cells with intensive increases in built-up areas occurred within the range of 15 km–30 km from the city center, while a large number of grid cells with intense but small increases in built-up areas occurred between 10 km and 20 km, similar to the last period (Fig. 6(d)). The intense but small increases can be understood as an infilling urbanization process. Different from horizontal urban growth, most grid cells with a large increase in MTB areas occurred in the 5–15 km range, and then expanded to longer distances (to 10 km and even 20 km) (Fig. 6(g) and (j)). In addition, the greater value ranges of the increases in built-up areas (200–800 pixels) and MTB areas (20–80 pixels) show that there was an outward expanding trend (Fig. 6(a), (d), (g), and (j)), which indicates that intense urbanization and infilling urbanization processes tended to spread out from the center.

In the urban area of Seoul, widespread urban growth happened in both horizontal and vertical dimensions (Fig. 6(b), (e), (h), and (k)). For the entire study period, most urban growth occurred within the 5–15 km range. Intense horizontal urban growth occurred in the 10–17 km range during 1988–2002 and in the 12–17 km range during 2002–2015; growth in the first period was much stronger than in the second period, which may be explained by the high rate of urbanization and limited city size. MTB area growth mainly happened in the range of 5–15 km, and the growth in the second period was much stronger than in the first period (Fig. 6(h) and (k)).

Different from the two megacities described above, the horizontal urban growth in Tokyo occurred within two distance ranges, 5–15 km and 30–50 km, (Fig. 6(c) and (f)), with the first range representing the surrounding areas (mainly the southeastern corner) of the city center and the second range representing the western region of the city. During the study period, horizontal urban growth mainly occurred in the second range. In contrast, MTB growth in Tokyo mainly took place around the city center in a range of 0–20 km (around the first range), although low intensity MTB growth occurred in the whole city over the two periods (Fig. 6(i) and (l)).

4.3.2. Transition from non-MTB areas to MTB areas

Fig. 7 shows the transition status from non-MTB areas to MTB areas in 990 m × 990 m grid cells under different urbanization situations (i.e., different built-up area densities). Overall, MTBs tended to be built in highly urbanized areas (e.g., where built-up areas account for 90–100% of the total area of a grid cell) (Fig. 7). In Beijing, the increase of MTBs during 1989–2001 mainly occurred to renew old built-up areas with low buildings during an urban renewal process (Fig. 7(a)). However, the increase of MTBs in the period of 2001–2014 had relatively larger proportions occurring in less urbanized areas (Fig. 7(d)), showing an outward expanding trend (Fig. 5(a)); this feature may be explained by the relatively low development density of Beijing in 1989 compared with the other two cities (Figs. 4 and 5). Compared to the period of 2002–2015, the increase of MTBs in Seoul during 1988–2002 had a relatively larger proportion occurring in less urbanized areas (Fig. 7(b)), which illustrates that the horizontal urban expansion process in Seoul during that period took place with a relatively larger proportion being in the form of MTBs. During the period of 2002–2015, the increase of MTBs in Seoul tended to occur in more urbanized areas (Fig. 7(e)). Tokyo was already well-urbanized and densely developed before 1990 and thus had very limited horizontal expansion during the two studied periods (Fig. 4(c)). Therefore, vertical urban growth in Tokyo mainly happened in high-density development areas (Fig. 7(c) and (f)).

4.3.3. Developable spaces for horizontal and vertical urban growth

Fig. 8 shows the developable spaces for horizontal and vertical urban expansion in the three megacities in the late 1980s, that is, the original statuses of urban expansion in this study. It can be seen that while Beijing still had a large area of developable space for horizontal urban growth in 1989, Seoul and Tokyo had already been almost fully developed, with only a very small area of developable space left for horizontal urban expansion in 1988 (see light green areas in Fig. 8(a), (c), and (e)). While all three cities still had large developable space for MTBs in the late 1980s (see dark green areas in Fig. 8(b), (d), and (f)), very high buildings may not have been allowed to be built due to existing local policies in some areas, such as the area surrounding the Forbidden City in Beijing. Fig. 9 shows that all the studied megacities had more or less horizontal urban growth and vertical urban growth within their respective previously-developable spaces during the

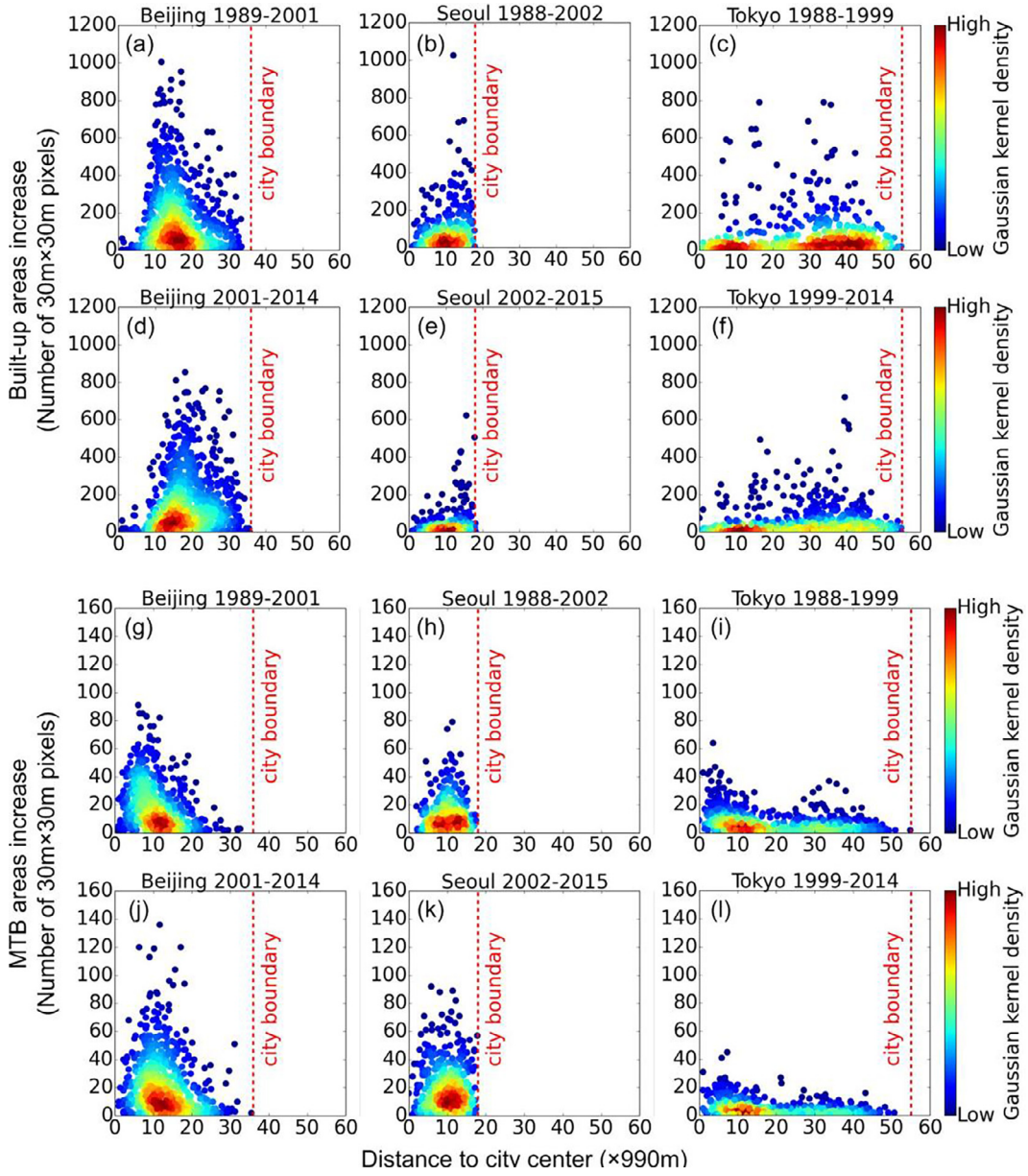

Fig. 6. Intensity visualization of horizontal and vertical urban expansion in the distance to city centers using Gaussian kernel density estimation. (a), (b), (c), (d), (e), and (f): Relationships between urban horizontal expansion and the distance to the city center in each study area for the corresponding studied period; (g), (h), (i), (j), (k), and (l): Relationships between vertical urban expansion and the distance to the city center in each study area for the corresponding studied period. It is worth noting that city boundaries (the red vertical dashed lines) are presented in order to visualize the relationships using the same distance scale. (For interpretation of the references to color in this figure legend, the reader is referred to the web version of this article.)

studied periods. However, the horizontal urban growth in Beijing is much clearer than in Tokyo and Seoul, and the vertical urban growth in Tokyo is very subtle compared with that in the other two cities. It is surprising that Seoul had a fast vertical urban growth rate during 2002–2015 while its population had almost no increase during this period.

In terms of development stages and patterns, Seoul and Tokyo tend to be similar. At the beginning (i.e., around 1988) of the studied period, the three cities had different development density levels, with the built-up area percentage being 36.3% for Beijing, 73.3% for Seoul, and 83.0% for Tokyo (Table 5). Both built-up areas and MTB areas noticeably increased in Beijing during the two studied periods. In Seoul, horizontal urban growth slowed down as vertical urban growth greatly increased with time, probably because its limited developable space for horizontal urban growth pushed the urban expansion process more strongly toward vertical growth (Fig. 9(b) and (e)) as a result of the strong demand for larger living spaces (i.e., large apartments) driven by rapidly increased family income. Urban growth in Tokyo showed a different pattern: while horizontal urban growth almost reached its ceiling (90%) slowly, vertical urban growth was minor (and slowed down) during the two studied periods (Fig. 9(c) and (f) and Table 5), probably due to its very slow population increase and slower family income increase.

5. Discussion

5.1. Has the urban growth of megacities in developed countries stagnated?

One can see in the analysis above that horizontal urban growth in Seoul and Tokyo was slow. This can be attributed to three main reasons: limited developable spaces (Fig. 9), slow or stagnant population increase, and governmental policies. For example, because the greenbelt

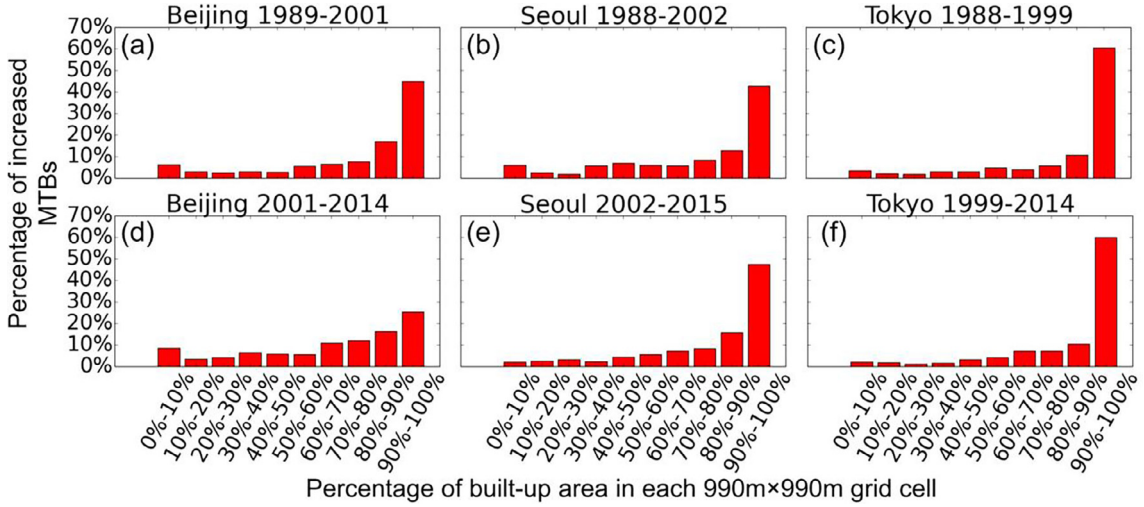

Fig. 7. Transition from non-MTB areas to MTB (mid-rise or taller building) areas: percentage of MTB increase during a time period versus percentage of built-up areas in grid cells at the beginning of the time period.

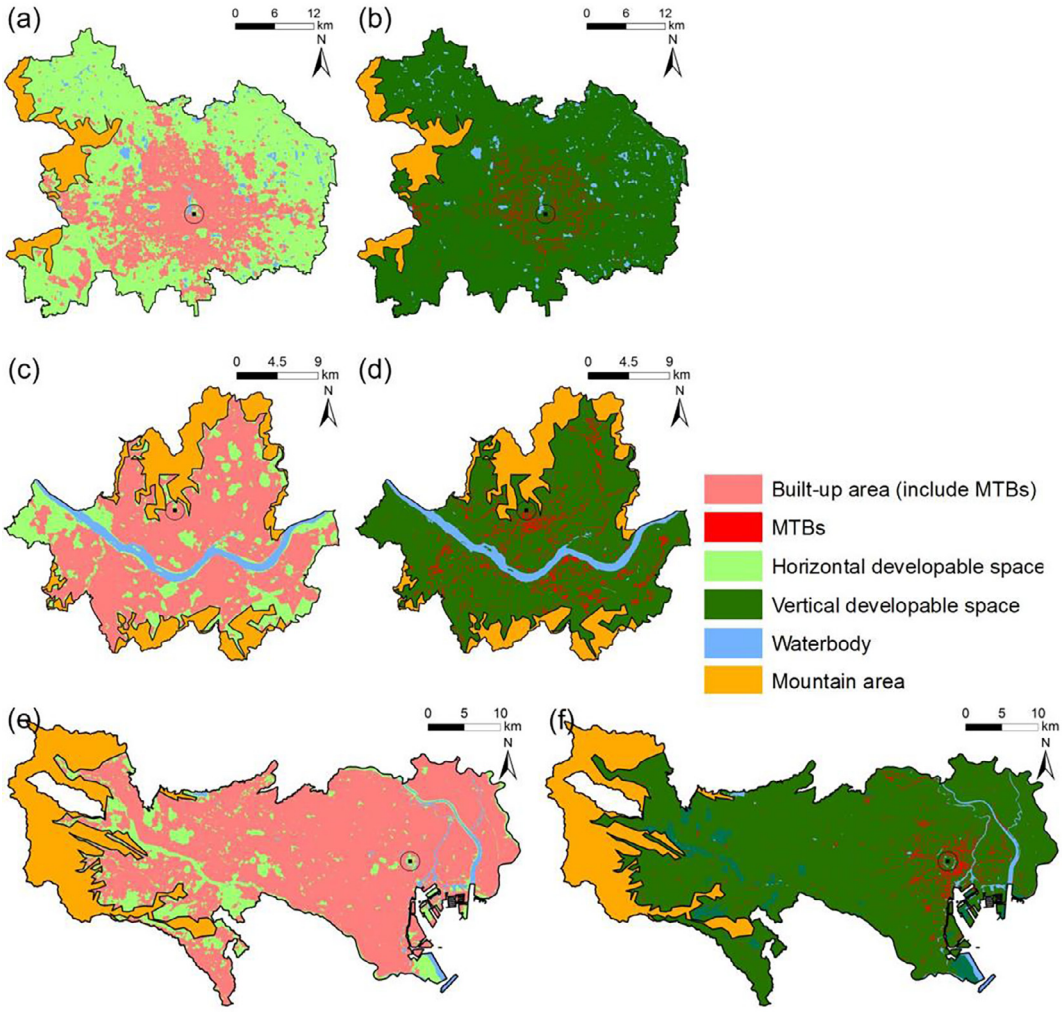

Fig. 8. Developable spaces for horizontal and vertical urban expansion in Beijing, Seoul, and Tokyo in the late 1980s. (a), (c), (e): Developable spaces for horizontal urban expansion in Beijing in 1989, Seoul in 1988, and Tokyo in 1988, respectively. (b), (d), (f): Developable spaces for vertical urban expansion in Beijing in 1989, Seoul in 1988, and Tokyo in 1988, respectively.

policy is a promising way of sustainable urban development, many well-developed megacities (including Seoul and Tokyo) adopted it (Bae & Sellers, 2007; Jun & Hur, 2001; Masucci, Stanilov, & Batty, 2013; Yokohari, Takeuchi, Watanabe, & Yokota, 2000). In Japan, a similar policy was enacted in 1968, which is called the City Planning Act (Saizen, Mizuno, & Kobayashi, 2006). While Beijing had a continuing

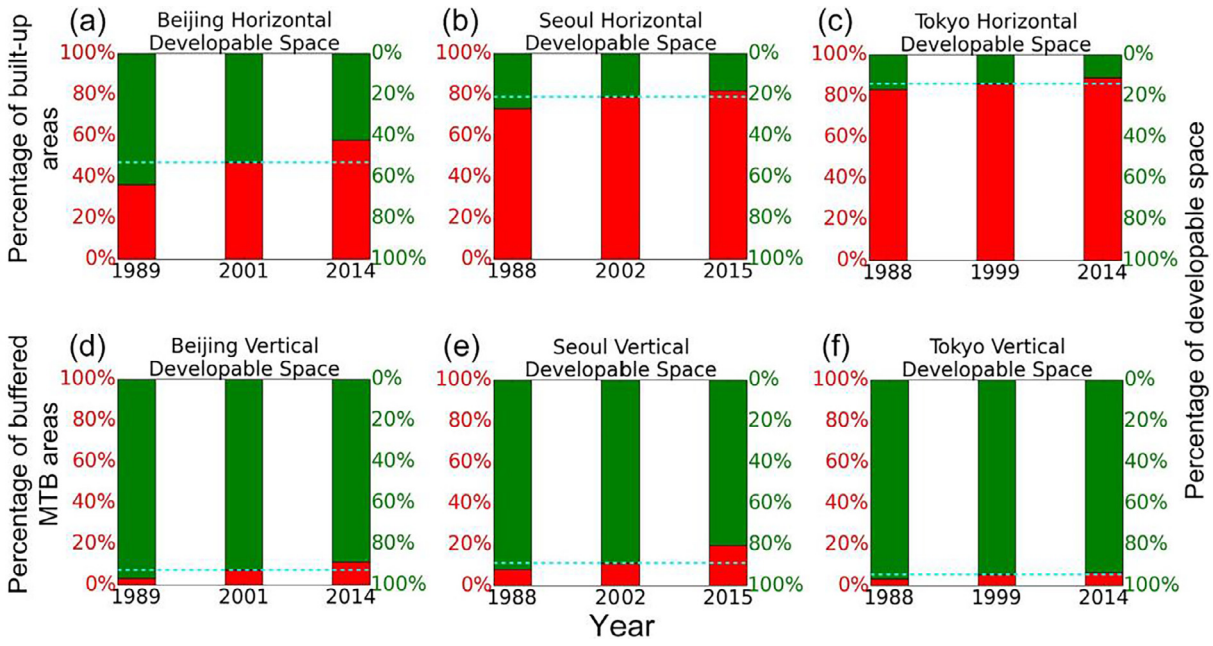

Fig. 9. Percentages of built-up areas, MTB areas, and developable spaces for horizontal and vertical urban expansion (red bars stand for developed areas; green bars stand for developable areas). Horizontal developable space includes vegetation areas and bare land within manually-drawn boundaries (i.e., non-built-up areas, non-waterbody, and non-mountainous areas). Vertical developable space includes horizontal developable space and built-up areas without buffered MTB areas within manually-drawn boundaries (i.e., excluding MTBs and their one pixel buffer areas). The y-axis in the first row (i.e., percentage of built-up area) indicates the percentage of built-up areas in terms of total area of horizontal developable and developed spaces; the y-axis in the second row indicates the percentage of MTB areas in terms of the total area of vertical developable and developed spaces. (For interpretation of the references to color in this figure legend, the reader is referred to the web version of this article.)

Table 5
Built-up areas, MTB areas, and their annual increases in developable space.

City name	Category	Percentage in total area of city (%)	Percentage in total area of city (%)	Annual increase from previous studied year (%)	Percentage in total area of city (%)	Annual increase from previous studied year (%)
Beijing	Year	1989	2001		2014	
	Built-up areas	36.3	47.0	0.9	57.9	0.8
	Buffered MTBs	3.4	7.2	0.3	11.2	0.3
Seoul	Year	1988	2002		2015	
	Built-up areas	73.3	78.9	0.4	81.8	0.2
	Buffered MTBs	8.0	11.1	0.2	19.7	0.7
Tokyo	Year	1988	1999		2014	
	Built-up areas	83.0	85.9	0.3	88.8	0.2
	Buffered MTBs	3.4	5.5	0.2	6.3	0.1

fast population increase during more than the last two decades, the population increases in Tokyo and Seoul were minor. However, this study provides evidence that regardless of urban planning policy, both Seoul and Tokyo were still growing vertically during the last two decades, despite very slow growth horizontally. The MTB percentage increase rate in Seoul during 2002–2015 was especially obvious (Table 5). This is consistent with the findings by Frolking et al. (2013), which showed that there was large vertical urban development in Seoul and Tokyo during 1999–2009.

5.2. *What are the similarities and differences in spatial patterns of horizontal and vertical urban growth between the studied megacities?*

In terms of the magnitude of horizontal urban growth, the growth of Beijing was much greater than that of the other two cities (Figs. 4(a), 5(a) and (d), and 9(a)) during the studied period, and Seoul was similar to Tokyo (Figs. 6(b), (e), (c), and (f), and 9(b) and (c)). This is because Beijing, as a relatively less developed megacity (development density 36.3% in 1989 and 57.9% in 2014, see Table 5), was going through a rapid urbanization process, while Tokyo and Seoul were already well-developed. As for the magnitude of vertical urban growth, Beijing had the largest MTB area increase (Fig. 6(g) and (j), Table 4). Beijing and Seoul had similar rates of MTB area increase for the period of around 2000 to around 2014 (Table 4), although the density of MTBs in Seoul was much higher than in Beijing (Fig. 9(d) and (e), Table 5). Tokyo had the lowest density of MTBs (Fig. 9(f)) and the least MTB area increase (Table 4). Similar to the situation in Seoul, MTB area increase in Tokyo mostly took place in a 5–15 km range during the study period (Fig. 6(h), (k), (i), and (l)).

The smallest horizontal urban growth in Tokyo, a highly-developed city even before 1988, can be partially explained by the urban development and sea reclamation in its Koto district. The vertical urban growth in Tokyo mainly occurred around its city center (Fig. 6(i) and (l)). Tokyo's urban landscape had been relatively stable (Ichikawa,

Okubo, Okubo, & Takeuchi, 2006), though an excessively high development density was still happening. The urbanization process in Seoul showed a relatively small horizontal urban expansion from 1988 to 2015 (Fig. 6(b) and (e)), but a great vertical urban growth as infilling, particularly for the period of 2002–2015 (Fig. 6(h) and (k)). The large vertical urban growth in Seoul during 2002–2015 may be caused by a strong demand for larger living apartments driven by a rapid increase in family income. Moreover, both Seoul and Tokyo had slow but widespread horizontal urban growth (Fig. 6(b), (e), (c), and (f)) when their development densities were high.

6. Conclusions

A spatial and temporal pattern analysis of the horizontal and vertical urban expansion of three megacities, Beijing, Seoul, and Tokyo, in East Asia during the late 1980s to the mid-2010s, is presented. Due to limited horizontal developable spaces, the horizontal urban growth in Seoul and Tokyo was very slow; however, Beijing expanded quickly in the horizontal dimensions during more than the last two decades while its land development density was low. The annual change rates in Beijing for the two periods showed an increasing trend in both horizontal and vertical urban growth. On the contrary, the change trend in horizontal and vertical urban growth in Tokyo for the two periods was decreasing, which might be because of the limited horizontal developable space and the slowing urban development process in the city. While the horizontal developable space in Seoul was similarly limited as in Tokyo, Seoul had a slow horizontal urban expansion progress, especially for the later period. However, Seoul increased largely in the vertical dimension over time in order to respond to the pressure of the limited horizontal developable space and the demand for building living areas. Overall, this study shows that: (1) both horizontal and vertical urban expansion had been happening in the megacities during the studied period; (2) different cities showed some differences in growth patterns because they were at different urban development stages and their urban expansion patterns were impacted by different geographical settings, population changes, and urban development policies; and (3) a similarity is that those megacities tended to horizontally expand initially and then grow vertically in the already developed areas.

With its novel findings this study may provide a useful new perspective on the urban expansion of megacities. It is useful for improving our understanding of the spatial and temporal patterns of urban expansion. Since urban growth and spatial patterns interact with socioeconomic, political, and urban environmental conditions, this study may also be helpful for understanding the environmental effects of urban expansion and providing support to sustainable urban development planning and policies for East Asia's megacities.

Acknowledgements

The authors would like to thank Krista Rogers for her helpful reviews of this manuscript. This work was supported in part by the U.S. National Science Foundation under Grant 1414108.

References

Alberti, M. (2005). The effects of urban patterns on ecosystem function. *International Regional Science Review, 28*(2), 168–192.
Angel, S., Parent, J., Civco, D. L., Blei, A., & Potere, D. (2011). The dimensions of global urban expansion: Estimates and projections for all countries, 2000–2050. *Progress in Planning, 75*(2), 53–107.
Bae, Y., & Sellers, J. M. (2007). Globalization, the developmental state and the politics of urban growth in Korea: A multilevel analysis. *International Journal of Urban and Regional Research, 31*(3), 543–560.
Bagan, H., & Yamagata, Y. (2012). Landsat analysis of urban growth: How Tokyo became the world's largest megacity during the last 40 years. *Remote Sensing of Environment, 127*, 210–222.
Bagan, H., & Yamagata, Y. (2014). Land-cover change analysis in 50 global cities by using a combination of Landsat data and analysis of grid cells. *Environmental Research Letters, 9*(6), 064015.
Beijing Statistical Bureau (2015). *Beijing statistical yearbook 2015 (in Chinese)*. Beijing: China Statistical Press.
Cho, C. J. (2002). The Korean growth-management programs: Issues, problems and possible reforms. *Land Use Policy, 19*(1), 13–27.
Chung, U., Choi, J., & Yun, J. I. (2004). Urbanization effect on the observed change in mean monthly temperatures between 1951–1980 and 1971–2000 in Korea. *Climatic Change, 66*(1–2), 127–136.
Civerolo, K., Hogrefe, C., Lynn, B., Rosenthal, J., Ku, J. Y., Solecki, W., et al. (2007). Estimating the effects of increased urbanization on surface meteorology and ozone concentrations in the New York City metropolitan region. *Atmospheric Environment, 41*(9), 1803–1818.
Doxani, G., Karantzalos, K., & Tsakiri-Strati, M. (2012). Monitoring urban changes based on scale-space filtering and object-oriented classification. *International Journal of Applied Earth Observation and Geoinformation, 15*, 38–48.
Frolking, S., Milliman, T., Seto, K. C., & Friedl, M. A. (2013). A global fingerprint of macro-scale changes in urban structure from 1999 to 2009. *Environmental Research Letters, 8*(2), 024004.
Han, J., Hayashi, Y., Cao, X., & Imura, H. (2009). Application of an integrated system dynamics and cellular automata model for urban growth assessment: A case study of Shanghai, China. *Landscape and Urban Planning, 91*(3), 133–141.
Hara, Y., Takeuchi, K., & Okubo, S. (2005). Urbanization linked with past agricultural landuse patterns in the urban fringe of a deltaic Asian mega-city: A case study in Bangkok. *Landscape and Urban Planning, 73*(1), 16–28.
Hasegawa, T. (2013). *Introduction to the building standard law-building regulation in Japan*. The building Center of Japan.
Huang, J., Lu, X. X., & Sellers, J. M. (2007). A global comparative analysis of urban form: Applying spatial metrics and remote sensing. *Landscape and Urban Planning, 82*(4), 184–197.
Hung, W. C., Chen, Y. C., & Cheng, K. S. (2010). Comparing landcover patterns in Tokyo, Kyoto, and Taipei using ALOS multispectral images. *Landscape and Urban Planning, 97*(2), 132–145.
Ichikawa, K., Okubo, N., Okubo, S., & Takeuchi, K. (2006). Transition of the satoyama landscape in the urban fringe of the Tokyo metropolitan area from 1880 to 2001. *Landscape and Urban Planning, 78*(4), 398–410.
Jones, E., Oliphant, T., & Peterson, P. (2016). *SciPy: Open source scientific tools for Python. 2001*. URL http://www.scipy.org.
Jun, M. J., & Hur, J. W. (2001). Commuting costs of "leap-frog" newtown development in Seoul. *Cities, 18*(3), 151–158.
Kim, I. K. (2010). Socioeconomic concentration in the Seoul metropolitan area and its implications in the urbanization process of Korea. *Korean Journal of Sociology, 44*(3), 111–128.
Kim, M. K., & Kim, S. (2011). Quantitative estimates of warming by urbanization in South Korea over the past 55 years (1954–2008). *Atmospheric Environment, 45*(32), 5778–5783.
Kontgis, C., Schneider, A., Fox, J., Saksena, S., Spencer, J. H., & Castrence, M. (2014). Monitoring peri-urbanization in the greater Ho Chi Minh City metropolitan area. *Applied Geography, 53*, 377–388.
Kuang, W., Chi, W., Lu, D., & Dou, Y. (2014). A comparative analysis of megacity expansions in China and the US: Patterns, rates and driving forces. *Landscape and Urban Planning, 132*, 121–135.
Lampe, O. D., & Hauser, H. (2011). Interactive visualization of streaming data with kernel density estimation. In *Pacific visualization symposium (PacificVis)*, 2011 IEEE (pp. 171–178).
Lee, D., & Choe, H. (2011). Estimating the impacts of urban expansion on landscape ecology: Forestland perspective in the greater Seoul metropolitan area. *Journal of Urban Planning and Development, 137*(4), 425–437.
Leichtle, T., Geiß, C., Wurm, M., Lakes, T., & Taubenböck, H. (2017). Unsupervised change detection in VHR remote sensing imagery – An object-based clustering approach in a dynamic urban environment. *International Journal of Applied Earth Observation and Geoinformation, 54*, 15–27.
Li, W. (2007). Markov chain random fields for estimation of categorical variables. *Mathematical Geology, 39*(3), 321–335.
Li, W., & Zhang, C. (2008). A single-chain-based multidimensional Markov chain model for subsurface characterization. *Environmental and Ecological Statistics, 15*(2), 157–174.
Li, W., Zhang, C., Willig, M. R., Dey, D. K., Wang, G., & You, L. (2015). Bayesian Markov chain random field cosimulation for improving land cover classification accuracy. *Mathematical Geosciences, 47*(2), 123–148.
Luck, M., & Wu, J. (2002). A gradient analysis of urban landscape pattern: A case study from the Phoenix metropolitan region, Arizona, USA. *Landscape Ecology, 17*(4), 327–339.
Masucci, A. P., Stanilov, K., & Batty, M. (2013). Limited urban growth: London's street network dynamics since the 18th century. *PLoS ONE, 8*(8), e69469.
Montgomery, M. R. (2008). The urban transformation of the developing world. *Science, 319*(5864), 761–764.
Murakami, A., Zain, A. M., Takeuchi, K., Tsunekawa, A., & Yokota, S. (2005). Trends in urbanization and patterns of land use in the Asian mega cities Jakarta, Bangkok, and Metro Manila. *Landscape and Urban Planning, 70*(3), 251–259.
Pan, X. Z., Zhao, Q. G., Chen, J., Liang, Y., & Sun, B. (2008). Analyzing the variation of building density using high spatial resolution satellite images: The example of Shanghai City. *Sensors, 8*(4), 2541–2550.
Saizen, I., Mizuno, K., & Kobayashi, S. (2006). Effects of land-use master plans in the metropolitan fringe of Japan. *Landscape and Urban Planning, 78*(4), 411–421.
Salvati, L., Zitti, M., & Sateriano, A. (2013). Changes in city vertical profile as an indicator

of sprawl: Evidence from a Mediterranean urban region. *Habitat International, 38*, 119–125.
Schneider, A. (2012). Monitoring land cover change in urban and peri-urban areas using dense time stacks of Landsat satellite data and a data mining approach. *Remote Sensing of Environment, 124*, 689–704.
Schneider, A., Chang, C., & Paulsen, K. (2015). The changing spatial form of cities in Western China. *Landscape and Urban Planning, 135*, 40–61.
Schneider, A., & Mertes, C. M. (2014). Expansion and growth in Chinese cities, 1978–2010. *Environmental Research Letters, 9*(2), 024008.
Schneider, A., Mertes, C. M., Tatem, A. J., Tan, B., Sulla-Menashe, D., Graves, S. J., et al. (2015). A new urban landscape in East-Southeast Asia, 2000–2010. *Environmental Research Letters, 10*(3), 034002.
Scott, D. W. (2015). *Multivariate density estimation: Theory, practice, and visualization.* John Wiley & Sons.
Seoul Statistics. (2016). Changes in population (Population Census) (in English). Available at: http://english.seoul.go.kr/get-to-know-us/statistics-of-seoul/seoul-statistics-by-category/#none. Accessed 16.11.27.
Statistics of Tokyo. (2016). Tokyo statistical yearbook (in English). Available at: http://www.toukei.metro.tokyo.jp/tnenkan/tn-eindex.htm#1985. Accessed 16.08.22.
Stone, B. (2008). Urban sprawl and air quality in large US cities. *Journal of Environmental Management, 86*(4), 688–698.
Sung, H., & Oh, J. T. (2011). Transit-oriented development in a high-density city: Identifying its association with transit ridership in Seoul, Korea. *Cities, 28*(1), 70–82.
Taubenböck, H., Esch, T., Felbier, A., Wiesner, M., Roth, A., & Dech, S. (2012). Monitoring urbanization in mega cities from space. *Remote Sensing of Environment, 117*, 162–176.
Taubenböck, H., Wegmann, M., Roth, A., Mehl, H., & Dech, S. (2009). Urbanization in India-Spatiotemporal analysis using remote sensing data. *Computers, Environment and Urban Systems, 33*(3), 179–188.
Taubenböck, H., Wiesner, M., Felbier, A., Marconcini, M., Esch, T., & Dech, S. (2014). New dimensions of urban landscapes: The spatio-temporal evolution from a polynuclei area to a mega-region based on remote sensing data. *Applied Geography, 47*, 137–153.
United Nations, D. E. S. A. (2015). World urbanization prospects: The 2014 revision.
World Bank Group (2015). *East Asia's changing urban landscape: Measuring a decade of spatial growth.* Washington, DC: Urban Development.
Wurm, M., Taubenböck, H., Esch, T., Fina, S., & Siedentop, S. (2013). The changing face of urban growth: An analysis using earth observation data. In *Proceedings of the IEEE Joint Urban Remote Sensing Event (JURSE)* (pp. 25–28), Sao Paulo, Brazil.
Yau, C.. R tutorial with Bayesian statistics using OpenBUGS. (2012). Available at: http://www.r-tutor.com/elementary-statistics/qualitative-data/relative-frequency-distribution-qualitative-data Accessed 16.08.22 .
Yokohari, M., Takeuchi, K., Watanabe, T., & Yokota, S. (2000). Beyond greenbelts and zoning: A new planning concept for the environment of Asian mega-cities. *Landscape and Urban Planning, 47*(3), 159–171.
Yu, B., Liu, H., Wu, J., Hu, Y., & Zhang, L. (2010). Automated derivation of urban building density information using airborne LiDAR data and object-based method. *Landscape and Urban Planning, 98*(3), 210–219.
Yu, X. J., & Ng, C. N. (2007). Spatial and temporal dynamics of urban sprawl along two urban–rural transects: A case study of Guangzhou, China. *Landscape and Urban Planning, 79*(1), 96–109.
Zhang, P. (2015). Spatiotemporal features of the three-dimensional architectural landscape in Qingdao, China. *PLoS ONE, 10*(9), e0137853.
Zhang, W., Li, W., & Zhang, C. (2016). Land cover post-classifications by Markov chain geostatistical cosimulation based on pre-classifications by different conventional classifiers. *International Journal of Remote Sensing, 37*(4), 926–949.
Zhang, W., Li, W., Zhang, C., & Li, X. (2017). Incorporating spectral similarity into Markov chain geostatistical cosimulation for reducing smoothing effect in land cover postclassification. *IEEE Journal of Selected Topics in Applied Earth Observations and Remote Sensing, 10*(3), 1082–1095.
Zhang, W., Li, W., Zhang, C., & Ouimet, W. (2017). Detecting horizontal and vertical urban growth from medium resolution imagery and its relationships with major socioeconomic factors. *International Journal of Remote Sensing, 38*(12), 3704–3734.